Hindawi
Geofluids
Volume 2018, Article ID 8321974, 8 pages
https://doi.org/10.1155/2018/8321974

Research Article

Characterization of Permeability Changes in Coal of High Rank during the CH_4-CO_2 Replacement Process

X. M. Ni[1,2] **Q. F. Jia**[1] **and Y. B. Wang**[3]

[1]*School of Energy Science and Engineering, Henan Polytechnic University, Jiaozuo, China*
[2]*Collaborative Innovation Center of Coalbed Methane and Shale Gas for Central Plains Economic Region, Henan Province, Jiaozuo, China*
[3]*College of Geoscience and Surveying Engineering, China University of Mining & Technology, Beijing, China*

Correspondence should be addressed to X. M. Ni; nxm1979@126.com

Received 12 July 2018; Accepted 10 September 2018; Published 12 November 2018

Academic Editor: Julie K. Pearce

The influences of coal matrix expansion/contraction and effective stress on the permeability of coal with different thermal maturities are different during the CH_4-CO_2 replacement process due to different mechanical properties and gas adsorption capacities. To accurately predict the variation law of coal permeability during the CH_4-CO_2 replacement process, it is critical to understand how the matrix expansion/contraction and effective stress affect the permeability of coal at different thermal maturities during the CH_4-CO_2 replacement. In this study, the permeability of two coal specimens with anthracite and high-rank bituminous coal during the CH_4-CO_2 replacement process under different confining and injection pressures was tested using a CBM replacement testing machine. The results demonstrate that with decreasing gas injection pressure, the permeability of the two coal specimens exhibited a U-shaped correlation under different confining pressures. Under the same gas injection pressure, with increasing effective stress, the permeability presented a negative exponential decrease and the permeability of the anthracite decreased more significantly. Moreover, under the same confining pressure, with increasing gas injection pressure, the decreasing permeability agreed with Langmuir curve and the permeability of high-rank bituminous coal was more significantly reduced.

1. Introduction

Coal has a greater adsorption capacity for CO_2 compared to CH_4 under the same conditions [1, 2]. It has been shown to be feasible to replace CH4 from coal seams by means of competitive adsorption of CO_2 [3–5]. However, due to gas adsorption/desorption and gas pressure changes during the replacement process, the permeability of the coal always undergoes complex changes due to the synergetic effects of coal matrix expansion/contraction and effective stress. Extensive studies have been made aiming at understanding how the matrix expansion/contraction and effective stress impact the permeability during the replacement.

Many studies have shown that as the amount of swelling of coal adsorbed with CO_2 is greater than that of CH_4 under the same conditions [6–8], the permeability of coal specimens decreases during the CH_4-CO_2 replacement process [5, 9–11]. To investigate the amount of swelling of coal after absorbing gas, a number of approaches including probe test methods [12–14], stress detectors [15–17], and fiber optic cameras [18–21] have been adopted by some researchers. Data from these studies show that the amount of swelling and adsorption capacity are in close agreement with the results of the Langmuir adsorption isotherm. Some applied theories including adsorption isotherms, surface free energy, elastic-plastic mechanics, and the stress-strain relationship of coal rock have been used to construct mathematic models of swelling and shrinkage for coal matrix after adsorbing/desorbing gas [22, 23]. The effective stress during the gas injection process has also been shown to change.

To investigate the impact of varying effective stresses on the permeability of coal, studies have suggested improved rock mechanics and servo-controlled testing systems to conduct pressure and flow tests. The study results have indicated that as effective stress increases, permeability shows a negative exponential decay [24–27]. Each of the previously mentioned

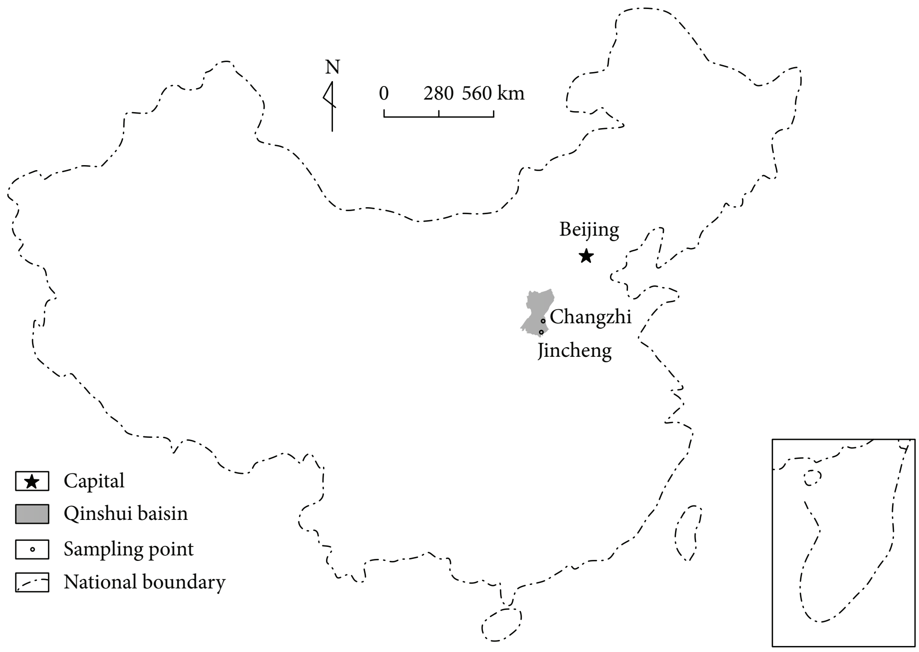

FIGURE 1: Location of coal specimens studied in this paper.

studies analyzed coal matrix expansion/contraction or effective stress and did not comprehensively consider the relationship between the two. Hence, previous studies are limited in revealing the impact of effective stress and matrix expansion/contraction on the permeability of coal during the CH_4-CO_2 replacement process.

This research aimed at testing the contribution of matrix expansion and effective stress changes on the permeability of coal with different metamorphic degrees during the CH_4-CO_2 replacement process. For this purpose, the change laws of permeability of anthracite and high-rank bituminous coal specimens during the replacement process were analyzed under varying confining and gas injection pressures. The results provide a theoretical foundation for in situ CO_2 injection.

2. Experimental Methods

2.1. Preparation of Coal Specimens and Experimental Device. Coal specimens with different thermal maturities were obtained from the Sihe and Tunliu coal mines in the Qinshui Basin of Shanxi Province of China. Location of coal specimens is shown in Figure 1. Prior to the experiment, the vitrinite reflectance, proximate analysis, adsorption constant, and elastic modulus of the coal specimens were determined, and the results are summarized in Tables 1 and 2. Cylindrical core specimens 50 mm in diameter and 100 mm in length were specimend from the coal block in the direction parallel to the bedding planes, as shown in Figure 2. According to Table 1, the vitrinite reflectance of the specimens from the Sihe and Tunliu coal mines were 3.07% and 1.96%, respectively.

Based on the classification of *ISO 11760 Classification of coal*, the coal specimens from the Sihe and Tunliu mines were anthracite and meager lean coal. In the following statement, the Sihe and Tunliu specimens are, respectively, represented by anthracite (HA) and high-rank bituminous coal (HB). As shown in Table 2, when the temperature of the test was set to 298.15 K, the adsorption capability and elastic modulus of the coal specimens from the Sihe coal mine were both greater than those from the Tunliu mine.

TABLE 1: Results of vitrinite reflectance and proximate analysis.

Coal specimen	Length (mm)	Diameter (mm)	R_O, ran (%)	M_{ad}	A_{ad}	V_{ad}
Sihe	98.63	49.16	3.07	1.76	14.74	5.63
Tunliu	102.12	49.22	1.96	5.02	14.85	11.97

[a] M_{ad} = moisture content (wt.%, air dry basis), A_{ad} = ash yield (wt.%, air dry basis), and V_{ad} = volatile matter (wt.%, air dry basis).

The CBM replacement testing machine in the National Engineering Research Center of Coalbed Methane Development & Utilization, Beijing, was used as the experimental device. This device was used to test the change in permeability of the specimens under different stresses and gas injection pressures. The working mechanism can be described as (1) a stress-loading device was used to apply confining pressure and axial compression on the coal specimens by simulating stress states of the specimens; (2) gas pipes on both ends of the specimens were connected to the devices including a metering pump, a flow rate controller, a flow meter, and a pressure gauge. Gas was injected with the coal specimens under different pressures. The corresponding data were collected and used to calculate the permeability, as shown in Figure 3.

The parameters in the experiment included as follows: the dimension was set to be ¢50 × 100 mm or ¢25 × 50 mm, the temperature ranged between 173.15~373.15 K with a

Table 2: Testing results of isothermal adsorption experiments about CO_2 and CH_4.

Specimens	Adsorption constants of CO_2		Adsorption constants of CH_4		Density (kg/m^3)	Matrix elastic modulus (GPa)	Testing temperature (K)
	V_L(m^3/t)	P_L/MPa	V_L(m^3/t)	P_L/MPa			
Sihe	16.81	0.78	12.12	1.53	1462	5.209	298.15
Tunliu	16.08	1.32	5.47	2.86	1436	5.612	298.15

(a) (b)

Figure 2: Photo of prepared specimens. (a) Tunliu specimen. (b) Sihe specimen.

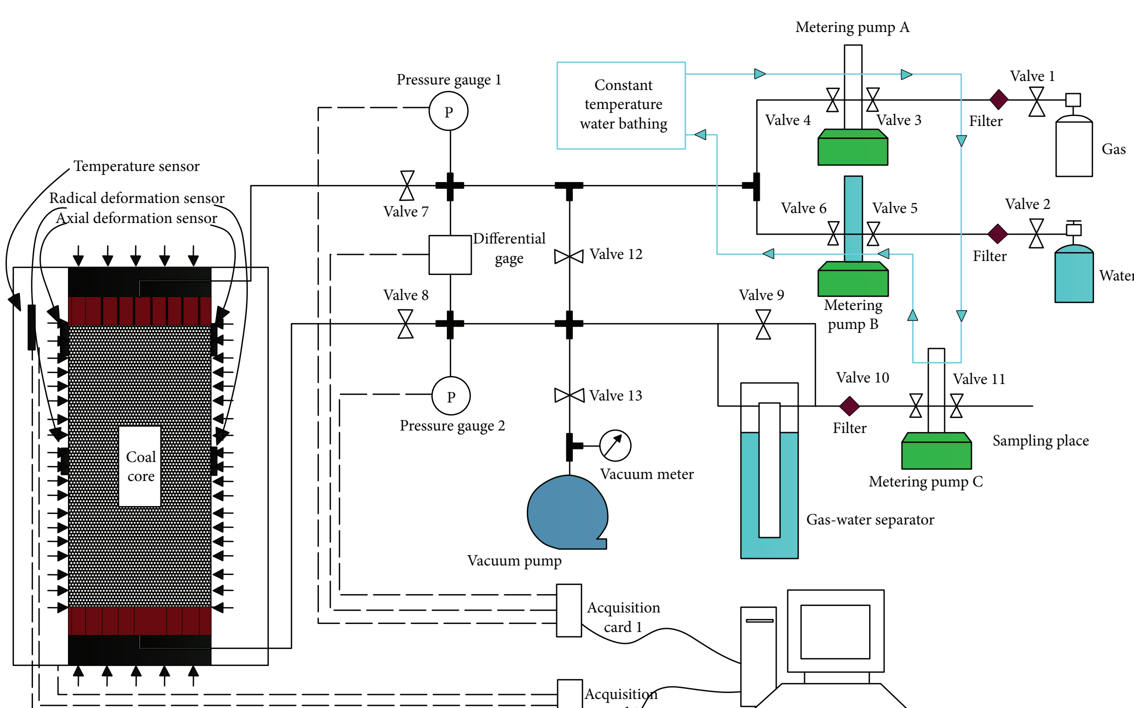

Figure 3: Working principle of mixed gas displacement testing machine.

precision of ±0.1 K, and the confining pressure was in the range of 0~30 MPa with a precision of ±0.5%. The gas injection pressure ranged between 0~20 MPa with a precision of ±0.5% FS, and the axial stress was in the range of 0~150 MPa with a precision of ≤±1%. Permeability ranged between 0.001~100 mD.

2.2. Experimental Procedure

(1) The gas pipelines were connected to examine the closure of the system, and the volume of the pipelines was tested. The HA coal specimen was dried and installed within a heat-shrinkable sleeve before being precisely put into the coal specimen chamber. Finally, the experimental system was performed by a vacuum pump

(2) After placing the specimens in a designed location as described, axial compression was applied to the specimen. Axial compression and confining pressure were alternatively loaded on the specimen until the confining pressure reached up to 6 MPa. To prevent coal specimen from damage, the stress-loading speed was less than or equal to 0.2 MPa/s

(3) CH_4 was injected at a constant pressure of 1 MPa. As the adsorption of CH_4 reached equilibrium, CO_2 was injected at a higher pressure of 1.25 MPa to induce competitive adsorption. When the adsorption and desorption for both types of gas reached equilibrium, the pressure and gas flow rates on both ends of the specimen were recorded. The permeability of the coal specimens was calculated based on equation (1). Afterwards, gas injection was ceased. The experimental system has undergone sufficient vacuum-pumping.

$$K_{ge} = \frac{2 \times 10^2 p_d q_{ge} \mu_g h}{A\left(p_u^2 - p_d^2\right)}, \quad (1)$$

where K_{ge} is the effective permeability, mD; p_u and p_d are the fluid pressure on both ends of each specimen, MPa. q_{ge} refers to fluid velocity, cm^3/s; μ_g is the fluid viscosity, $mPa \cdot s$; h is the length of the specimens, cm; and A represents the cross-section area of each specimen, cm^2

(4) The permeability of HA coal specimen under different injection pressures (1.25, 2.25, 3.25, 4.25, and 5.25 MPa) under a confining pressure of 6 MPa was tested by repeating procedure (3)

(5) The permeability of the HA coal specimen under different confining pressures (6, 8, 10, 12, and 14 MPa) and different injection pressures (1.25, 2.25, 3.25, 4.25, 5.25, and 6.25 MPa) during the CH_4-CO_2 replacement process was tested by repeating procedures (2)~(4)

(6) The HA coal specimen was replaced by the HB coal specimen after the gas injection was ceased and stress was unloaded

(7) The permeability of the HB coal specimen under different confining pressures (8, 12, 16, and 20 MPa) and different injection pressures (1.25, 2.25, 3.25, 4.25, 5.25, and 6.25 MPa) during the CH_4-CO_2 replacement process was tested by repeating the above procedures

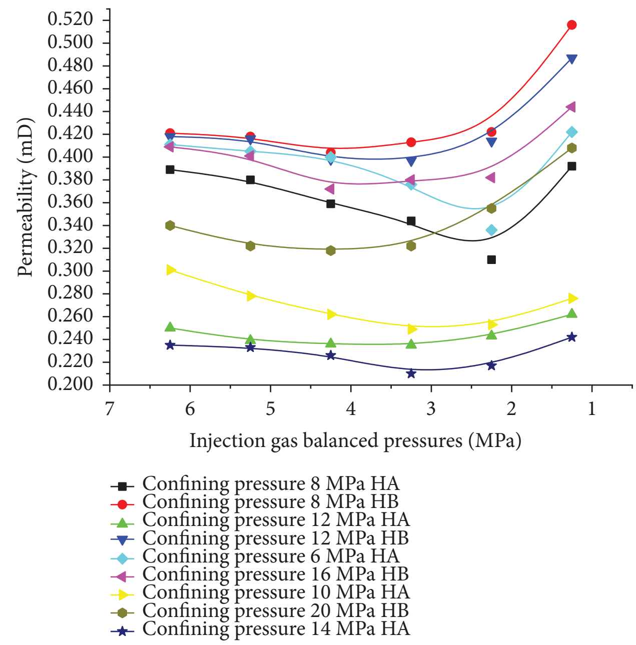

Figure 4: Permeability variation of the HA and HB coal specimens under different confining and injection pressures.

3. Results and Discussion

3.1. Experimental Results. The change in permeability of coal specimens during the CH_4-CO_2 replacement process under different confining pressures is shown in Figure 4.

Figure 4 shows that under different confining pressures and with decreasing gas injection pressure, the permeability of the two coal specimens all exhibited a U-shaped correlation. The greater the confining pressure, the lower the permeability of the same coal specimen. In the anthracite specimen, when the gas injection pressures were 1.3 and 6.25 MPa, the permeability values were equal. In the high-rank bituminous coal specimen, when the gas injection pressures were and 6.25 MPa, the permeability values were equal.

3.2. Discussion

3.2.1. The Influence of Effective Stress on Permeability during the CH_4-CO_2 Replacement Process. According to the experimental design, the permeability of the two specimens was, respectively, tested during the CH_4-CO_2 replacement process under different confining and gas injection pressures. Under the same confining pressure, the effective stress changes with changing injection pressure, which leads to failure to apply the variable selective control method to derive the relationships between effective stress and permeability. However, under the same gas injection pressure, the effect of gas adsorption on permeability could be considered equal. Based on these observations, the permeability data of the same gas injection pressure and different confining pressures were selected to obtain the variation law of permeability.

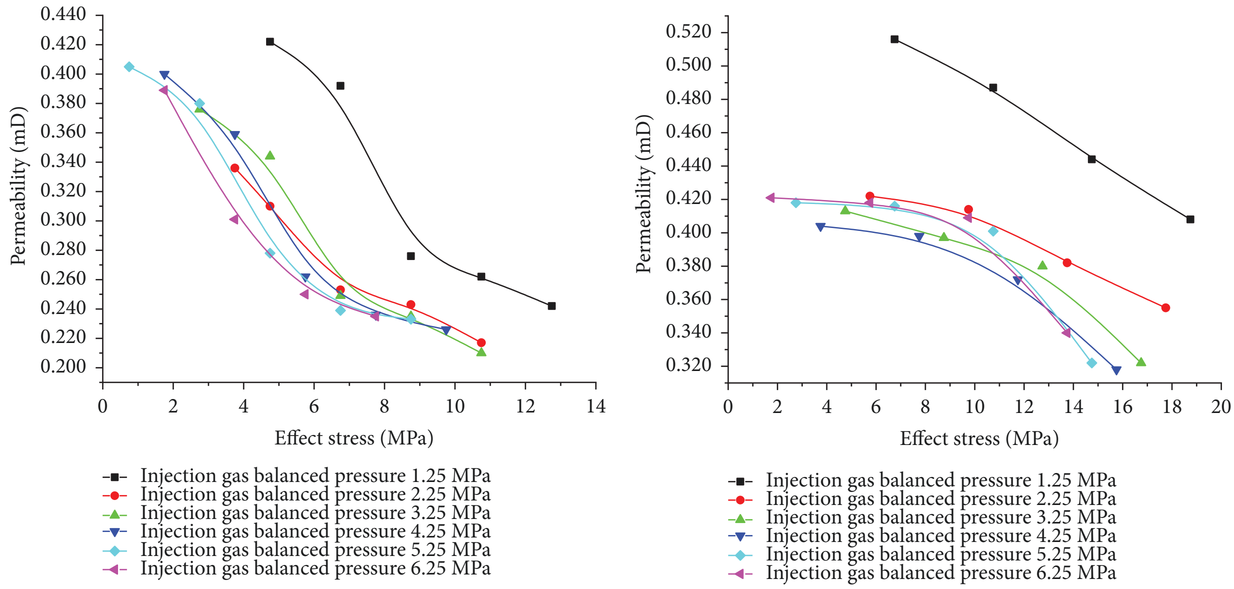

(a) HA coal

(b) HB coal

Figure 5: The change of permeability with a variation of effective stress.

Table 3: Contrasting results of the decreasing value of permeability caused by increasing effective stress on the HA and HB coal specimens.

Injection gas balanced pressures (MPa)	Relationships between effect stress and permeability		Decreasing values of permeability (mD)	
	HA coal	HB coal	HA coal	HB coal
1.25	$y = 0.609e^{-0.07x}$ $R^2 = 0.968$	$y = 0.595e^{-0.02x}$ $R^2 = 0.991$	0.180	0.107
2.25	$y = 0.410e^{-0.06x}$ $R^2 = 0.949$	$y = 0.467e^{-0.01x}$ $R^2 = 0.948$	0.119	0.067
3.25	$y = 0.464e^{-0.07x}$ $R^2 = 0.936$	$y = 0.465e^{-0.02x}$ $R^2 = 0.870$	0.166	0.091
4.25	$y = 0.452e^{-0.07x}$ $R^2 = 0.924$	$y = 0.449e^{-0.02x}$ $R^2 = 0.858$	0.174	0.086
5.25	$y = 0.433e^{-0.07x}$ $R^2 = 0.921$	$y = 0.463e^{-0.02x}$ $R^2 = 0.726$	0.172	0.096
6.25	$y = 0.431e^{-0.08x}$ $R^2 = 0.937$	$y = 0.449e^{-0.01x}$ $R^2 = 0.709$	0.154	0.081

Figure 5 shows the variation of permeability with increasing effective stresses during the CH_4-CO_2 replacement process at different gas injection pressures.

As can be seen in Figure 5, under different injection pressures, with increasing effective stress, the permeability of the HA coal decreases in a negative exponential manner and each of the correlation coefficients exceeds 0.9.

With increasing the effective stress, the permeability of the HB coal first slowly decreases and then presents a sharp decrease under the four gas injection pressures of 3.25, 4.25, 5.25, and 6.25 MPa. This indicates that the influence of effective stress on the permeability of HB coal exists at an abrupt turning point, after reaching a certain amount of adsorption; the greater the amount of gas adsorption, the earlier the turning point that permeability shows a sharp decrease. This may be related to the heterogeneity of the distribution of pores and fissures in coal.

To further study the change laws of permeability of the two specimens with a variation of effective stress, the decreased permeability caused by increased effective stress under the six injection gas balanced pressures was calculated, and the results are shown in Table 3.

As can be seen in Table 3, when the gas injection pressures are between 1.25 and 6.25 MPa, the decreasing values of permeability due to the increase of effective stress of HA coal range from 0.119 to 0.180 mD. For the HB coal, the values range from 0.067 to 0.107 mD, indicating that the permeability of the HA coal is more sensitive to effective stress.

3.2.2. Influence of Gas Adsorption/Desorption on Permeability during the CH_4-CO_2 Replacement Process. As the gas injection pressure changes, the permeability of the coal specimens also changed due to the gas adsorption/desorption. To study the change in permeability caused by gas adsorption as injection pressure increases, the value of permeability under the effect of gas adsorption was calculated. The calculation process is shown in equation 2.

$$K_a = K_b - K_c + K_e, \tag{2}$$

Table 4: Calculated results of permeability influenced by coal matrix shrinkage under different confining pressures.

Injection gas balanced pressures (MPa)	Permeability of coal specimens under the influence of coal matrix shrinkage (mD)								
	HA coal					HB coal			
	6 MPa	8 MPa	10 MPs	12 MPa	14 MPa	8 MPa	12 MPa	16 MPa	20 MPa
6.25	—	0.239	0.134	0.093	0.093	0.267	0.305	0.328	0.228
5.25	0.232	0.252	0.119	0.098	0.098	0.272	0.312	0.321	0.201
4.25	0.261	0.258	0.137	0.140	0.140	0.257	0.286	0.274	0.203
3.25	0.250	0.251	0.118	0.237	0.237	0.285	0.294	0.299	0.219
2.25	0.244	0.242	0.152	0.118	0.118	0.313	0.338	0.312	0.292
1.25	0.393	0.404	0.200	0.178	0.178	0.511	0.494	0.445	0.407

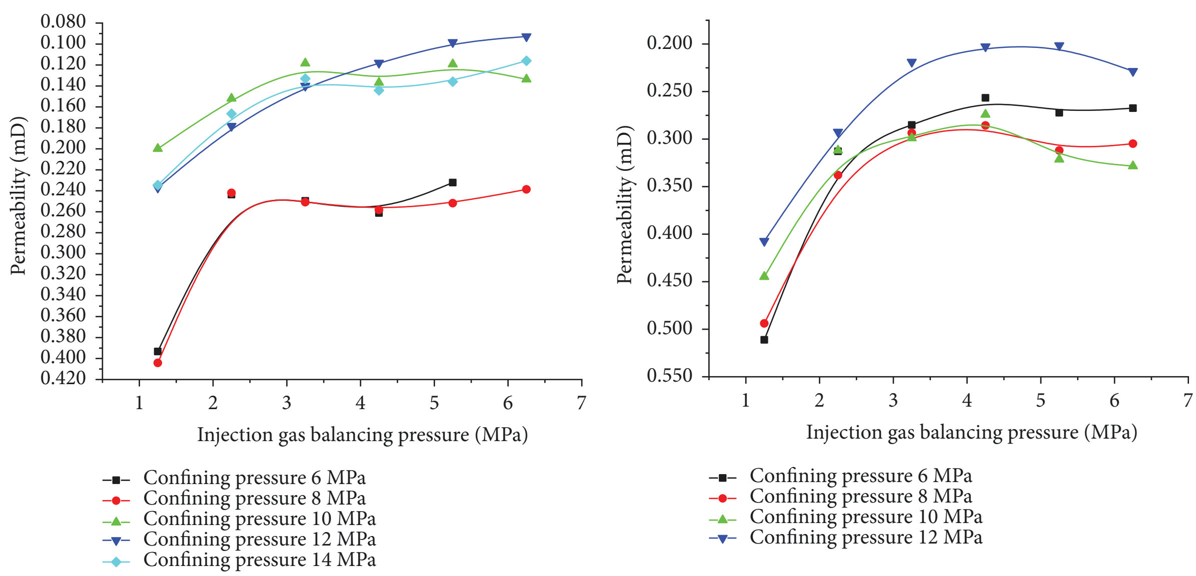

(a) HA coal

(b) HB coal

Figure 6: Permeability change characteristics due to gas desorption under different confining pressures.

where K_a is the permeability under the effect of gas adsorption, which can be seen as the original permeability of coal specimens plus the permeability change caused by effective stress gas and adsorption/desorption, mD; K_b is the permeability under the effect of gas adsorption and effective stress, which can be seen as the original permeability of coal specimens plus the permeability change caused by effective stress, mD; K_c is the permeability under the effect of effective stress, which can be seen as the original permeability of coal specimens plus the permeability change caused by effective stress gas and adsorption/desorption, mD; K_e is the original permeability of coal specimens.

As the experiment did not use inert gas to test the original permeability of the coal specimens, the permeability under an injection pressure of 1.25 MPa and the confining pressure of 0 MPa (calculated by the formula in Table 3) was considered as the original permeability. The permeability under the effects of gas adsorption was calculated, and the results are shown in Table 4.

According to the results shown in Table 4, the change in permeability under the effect of gas adsorption can be shown in Figure 6.

From Figure 6, it can be seen that under the different confining pressures, the permeability of both coal specimens showed a decreasing trend with increasing gas injection pressure. The shape of the permeability change curves are similar to that of the Langmuir adsorption, thus based on the calculated data in Table 4, the relationship between gas adsorption and permeability can be fitted by the following equation:

$$\frac{1}{K} = \frac{aP}{b+P}. \tag{3}$$

According to the Langmuir equation, K is the permeability of coal specimen, mD; P is the gas injection pressure, MPa; a is the lower boundary of permeability under the effect of gas adsorption, mD; b is the gas injection pressure on the half lower boundary, MPa.

Table 5 shows the fitting and the calculated results of permeability decrements under the effect of gas adsorption.

The a value represents the lower boundary of permeability under the effect of gas adsorption, as can be seen in Table 5; the a values in HA coal are smaller than those in the HB coal as a whole. On one hand, the original permeability

Table 5: Fitting and the calculated results of permeability increments under the effect of gas adsorption.

Confining pressure (MPa)	Coal thermal maturity	Fitting results a	b	R^2	Permeability decrement (mD)
6	HA	0.196	0.969	0.652	0.161
8	HA	0.187	0.826	0.617	0.166
8	HB	0.206	1.438	0.852	0.244
10	HA	0.106	0.938	0.657	0.066
12	HA	0.048	5.798	0.977	0.144
12	HB	0.248	0.965	0.742	0.189
14	HA	0.096	1.673	0.867	0.119
16	HB	0.270	0.58	0.423	0.117
20	HB	0.158	1.7	0.791	0.179

of the coal specimen is one of the most important reasons that led to the results. On the other hand, the differences of adsorption capacity are one of the important reasons; the greater the Langmuir volume, the lower the a values. The b values show no obvious regularity. Comparing the decrease of the permeability values caused by the gas adsorption of HA and HB coal, it can be concluded that in the replacement process, the effect of gas adsorption on the permeability of HB coal is greater than that of HA coal.

4. Conclusions

(1) With decreasing gas injection pressure, the permeability of the two coal specimens all tends to exhibit a U-shaped correlation under different confining pressures. When the gas injection pressure was reduced from 6.25 to 1.25 MPa, the permeability increase of HA coal ranged from −0.036 to 0.032 mD and that of the HB coal ranged from 0.035 to 0.095 mD. These data show that under the combined effect of effective stress and gas adsorption, the permeability of HB coal changes more than that of HA coal during the CH_4-CO_2 replacement process under the same conditions

(2) With increasing effective stress, the permeability decrease of HA coal ranged from 0.119 to 0.180 mD and that of HB coal ranged from 0.067 to 0.107 mD under different gas injection pressures. The permeability of HA coal decreased in a negative exponential manner, and the permeability of HB coal was not significantly affected by the effective stress in the lower effective stress range. However, when the effective stress reached the point of abrupt turning, the permeability begins to decrease drastically, indicating that during the replacement process, the effect of effective stress on the permeability of HA coal was greater than that of HB coal

(3) With increasing gas injection pressure, the curves of the change in permeability for the two specimens were similar to that of the Langmuir adsorption. The value of the Langmuir volume of coal determined the lower boundary of coal permeability affected by gas adsorption. With increasing gas adsorption, the permeability decrease of HA coal ranged from 0.066 to 0.161 mD and that of HB coal ranged from 0.117 to 0.244 mD under different effective stresses. These data indicate that during the replacement process, the effect of gas adsorption on the permeability of HB coal was greater than that of HA coal

Data Availability

The data of this manuscript is based on previous studies and obtained through experiments in the laboratory. Therefore, the data in this paper are all first-hand data, and the data are guaranteed to be true and reliable. In addition, some data have been confirmed at the CBM well site in Qinshui basin, China. In general, all the data in the paper are reliable.

Conflicts of Interest

The authors declare no competing financial interest.

Acknowledgments

This study is funded by Major National Oil and Gas Projects (2016ZX05066001-002), Program for Innovative Research Team in the University of Ministry of Education of China (IRT_16R22), Project of Innovation Talents in Colleges and Universities under contract support (15HASTIT050), and the Central Plains Economic Zone of coal seam gas (Ye Yan) Henan Collaborative Innovation Center support.

References

[1] C. M. White, D. H. Smith, K. L. Jones, A. L. Goodman, S. A. Jikich, and R. B. Lacount, "Sequestration of carbon dioxide in coal with enhanced coalbed methane recovery–a review," *Energy & Fuels*, vol. 19, pp. 559-560, 2005.

[2] F. Q. Zhang, G. X. Chen, K. H. Guo, and A. H. Do, "Process characteristics on replacement of bulk-methane hydrates with liquid cardon dioxide," *The Chinese Journal of Process Engineering*, vol. 18, pp. 639–645, 2018.

[3] L. E. Arri, Y. Dan, W. D. Morgan, and M. W. Jeansonne, "Modeling coalbed methane production with binary gas

sorption," in *SPE Rocky Mountain Regional Meeting*, pp. 459–472, Casper, WY, USA, May 1992.

[4] F. E. Hall, C. Zhou, K. A. M. Gasem, R. L. Robinson Jr., and Y. Dan, "Adsorption of pure methane, nitrogen, carbon dioxide and their mixtures on wet Fruitland coal," in *SPE Eastern Regional Meeting*, vol. 29, pp. 329–344, Charleston, WV, USA, November 1994.

[5] C. F. Hong and N. Liu, "Research progress in enhancement methods on replacement of CH4 from methane hydrate with CO_2," *Journal of Engineering for Thermal Energy & Power*, vol. 32, no. 1–6, p. 135, 2017.

[6] J. D. S. George and M. A. Barakat, "The change in effective stress associated with shrinkage from gas desorption in coal," *International Journal of Coal Geology*, vol. 45, no. 2-3, pp. 105–113, 2007.

[7] H. M. Yang, D. L. Xu, and L. W. Chen, "Quantitative study on displacement-replacement of methane in coal through CO2 injection," *Journal of Safety Science and Technology*, vol. 12, pp. 38–42, 2016.

[8] Z. Pan and L. D. Connell, "A theoretical model for gas adsorption-induced coal swelling," *International Journal of Coal Geology*, vol. 69, no. 4, pp. 243–252, 2007.

[9] S. Wong, D. Law, X. Deng, J. Robinson, B. Kadatz, and W. D. Gunter, "Enhanced coalbed methane and CO2 storage in anthracitic coals—Micro-pilot test at South Qinshui, Shanxi, China," *International Journal of Greenhouse Gas Control*, vol. 1, no. 2, pp. 215–222, 2007.

[10] T. Kiyama, S. Nishimoto, M. Fujioka, Z. Xue, Y. Ishijima, and Z. Pan, "Coal swelling strain and permeability change with injecting liquid/supercritical CO_2 and N_2 at stress-constrained conditions," *International Journal of Coal Geology*, vol. 85, no. 1, pp. 56–64, 2011.

[11] Z. Pan, L. D. Connell, and M. Camilleri, "Laboratory characterisation of coal reservoir permeability for primary and enhanced coalbed methane recovery," *International Journal of Coal Geology*, vol. 82, no. 3-4, pp. 252–261, 2010.

[12] X. M. Zhang, J. P. Li, Q. B. Wu, J. H. Nan, and L. Jiao, "Feasibility study on replacement of CH4 gas from methane hydrate with CO2 in frigid permafrost region," *Chemical Industry and Engineering Progress*, vol. 33, pp. 133–140, 2014.

[13] P. J. Reucroft and A. R. Sethuraman, "Effect of pressure on carbon dioxide induced coal swelling," *Energy & Fuels*, vol. 1, no. 1, pp. 72–75, 1987.

[14] P. L. Walker, S. K. Verma, J. Rivera-Utrilla, and M. R. Khan, "A direct measurement of expansion in coals and macerais induced by carbon dioxide and methanol," *Fuel*, vol. 67, no. 5, pp. 719–726, 1988.

[15] S. Majewska and J. Zietek, "Changes of acoustic emission and strain in hard coal during gas sorption–desorption cycles," *International Journal of Coal Geology*, vol. 70, no. 4, pp. 305–312, 2007.

[16] M. Ricaurte, C. Dicharry, X. Renaud, and J. P. Torre, "Combination of surfactants and organic compounds for boosting CO2 separation from natural gas by clathrate hydrate formation," *Fuel*, vol. 122, pp. 206–217, 2014.

[17] X. H. Fu, Y. Qin, B. Jiang, and W. F. Wang, "Study on mechanics experiments of multiphase medium coal rocks," *Acta Metallurgica Sinica*, vol. 8, pp. 446–452, 2002.

[18] Z. F. Wang, X. M. Sun, L. Tingkan, and H. Yabei, "Experiment research on strengthening gas drainage effect with fracturing technique by liquid CO_2 phase transition," *Journal of Henan Polytechnic University (Natural Science)*, vol. 34, pp. 1–5, 2015.

[19] S. Day, R. Fry, and R. Sakurovs, "Swelling of Australian coals in super-critical CO_2," *International Journal of Coal Geology*, vol. 74, no. 1, pp. 41–52, 2008.

[20] S. Durucan, M. Ahsan, and J. Q. Shi, "Matrix shrinkage and swelling characteristics of European coals," *Energy Procedia*, vol. 1, no. 1, pp. 3055–3062, 2009.

[21] Z. Z. Fang, X. C. Li, and B. Bai, "Study of method for simultaneously measuring adsorption deformation permeability of coal," *Chinese Journal of Rock Mechanics and Engineering*, vol. 28, pp. 1828–1833, 2009.

[22] X. M. Ni, C. C. Zhang, Y. B. Wang, and X. H. Wang, "Prediction of coal matrix shrinkage in gas-water two-phase flow stage," *Journal of China Coal Society*, vol. 39, Supplement 1, pp. 174–178, 2014.

[23] G. Z. Yin, W. P. Li, M. H. Li, X. Li, B. Z. Deng, and C. B. Jiang, "Permeability properties and effective stress of raw coal under loading-unloading conditions," *Journal of China Coal Society*, vol. 39, pp. 1497–1503, 2014.

[24] Y. Q. Hu, Y. S. Zhao, and J. P. Wei, "Experimental study of permeating law of coal mass gas under acting of three-dimensional stress," *Journal of Xi'an Mining Institute*, vol. 16, pp. 308–311, 1996.

[25] S. G. Cao, P. Guo, Y. Li, Y. J. Bai, Y. B. Liu, and J. Xu, "Effect of gas pressure on gas seepage of outburst coal," *Journal of China Coal Society*, vol. 35, pp. 595–599, 2010.

[26] J. Xu, J. Cao, B. Li, T. Zhou, M. Li, and D. Liu, "Experimental research on response law of permeability of coal to pore pressure," *Journal of Rock Mechanics and Engineering*, vol. 32, pp. 225–230, 2013.

[27] D. N. Espinoza and J. C. Santamarina, "P-wave monitoring of hydrate-bearing sand during CH_4–CO_2 replacement," *Journal of Natural Gas Science and Engineering*, vol. 5, no. 4, pp. 1031–1038, 2011.

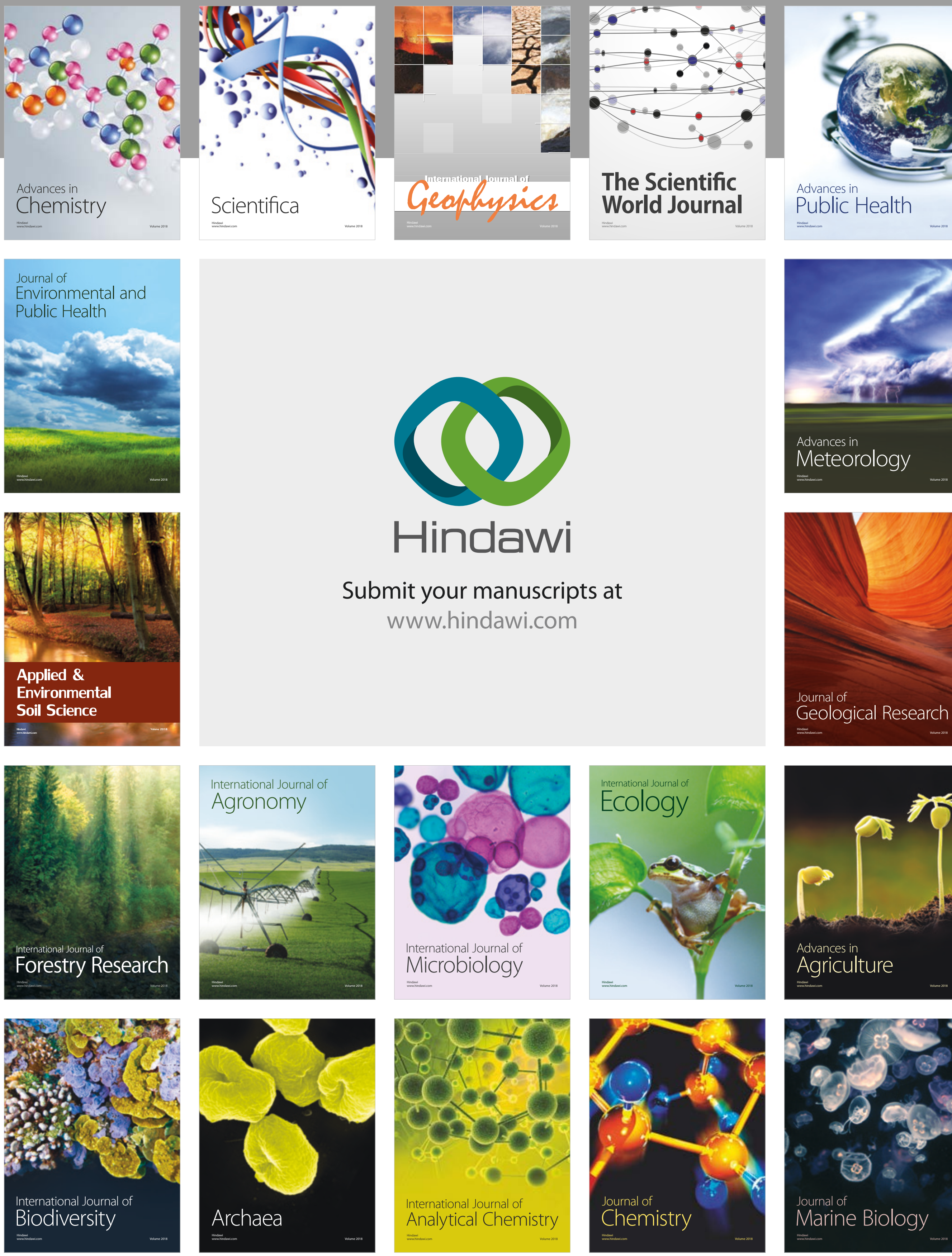
Advances in Chemistry
Scientifica
International Journal of Geophysics
The Scientific World Journal
Advances in Public Health
Journal of Environmental and Public Health
Hindawi
Submit your manuscripts at
www.hindawi.com
Advances in Meteorology
Applied & Environmental Soil Science
Journal of Geological Research
International Journal of Forestry Research
International Journal of Agronomy
International Journal of Microbiology
International Journal of Ecology
Advances in Agriculture
International Journal of Biodiversity
Archaea
International Journal of Analytical Chemistry
Journal of Chemistry
Journal of Marine Biology